Loading and Release Capabilities of Charged Dendronized Polymers Revealed by EPR Spectroscopy.

Dennis Kurzbach,[a] Daniel R. Kattnig,[a] Baozhong Zhang,[b] A. Dieter Schlüter[b] and Dariush Hinderberger[a]

[a] *Max Planck Institute for Polymer Research, Ackermannweg 10, 55128 Mainz, Germany; E-mail: dariush.hinderberger@mpip-mainz.mpg.de*
[b] *Department of Materials, Institute of Polymers, ETH Zurich, Wolfgang-Pauli-Str. 10, Zurich 8093, Switzerland*

Supporting Information

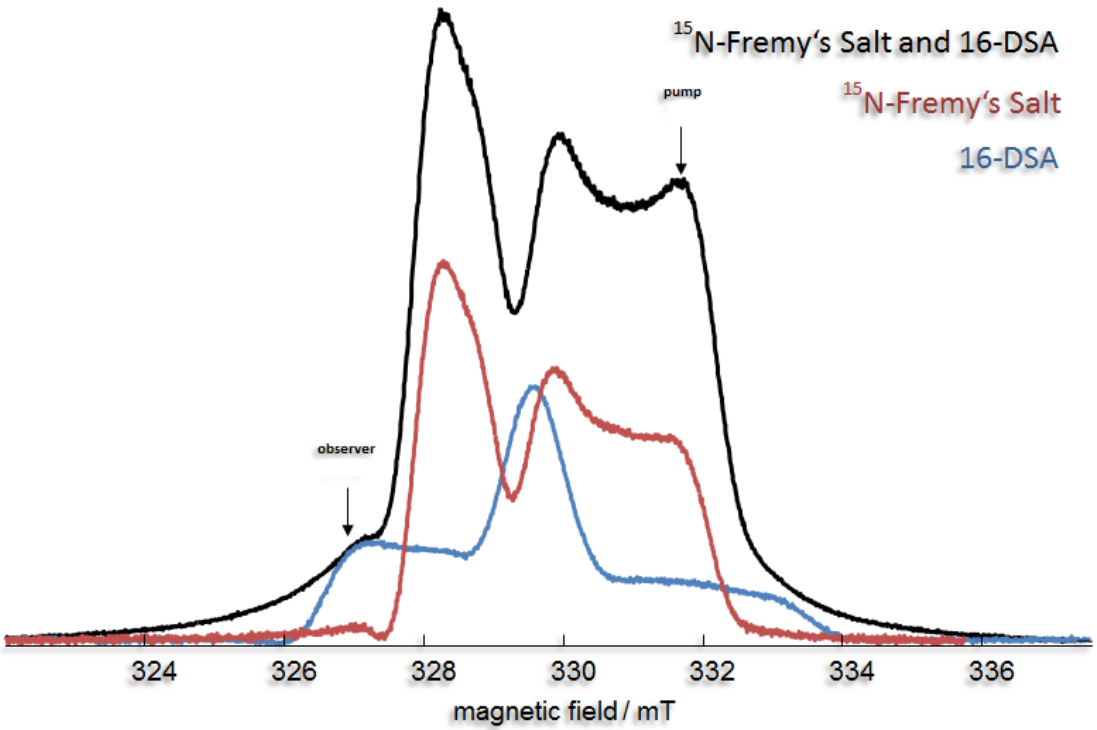

Figure S1. The electron spin echo (ESE) spectra of a 1mM solution of ^{15}N-Fremy's Salt (FS)), a 4 mM solution of 16-DSA (containing the nitroxide label with naturally abundant mixture of nitrogen isotopes, i.e. predominantly ^{14}N) , and a mixture of a 1 mM solution of ^{15}N-FS and a 4 mM solution of 16-DSA (black), all containing 4 wt % de-PG4 . The field position of the pump-pulse of the MISS-DEER experiment and the position of the observer-pulse are marked with arrows. In contrast to 5-DSA (Figure 2a)), a strong line broadening of the two-component spectra can be detected, which is most-likely the reason for 16-DSA being less prominent than 5-DSA in the bimodal spectrum (Figure 2a in the main manuscript).

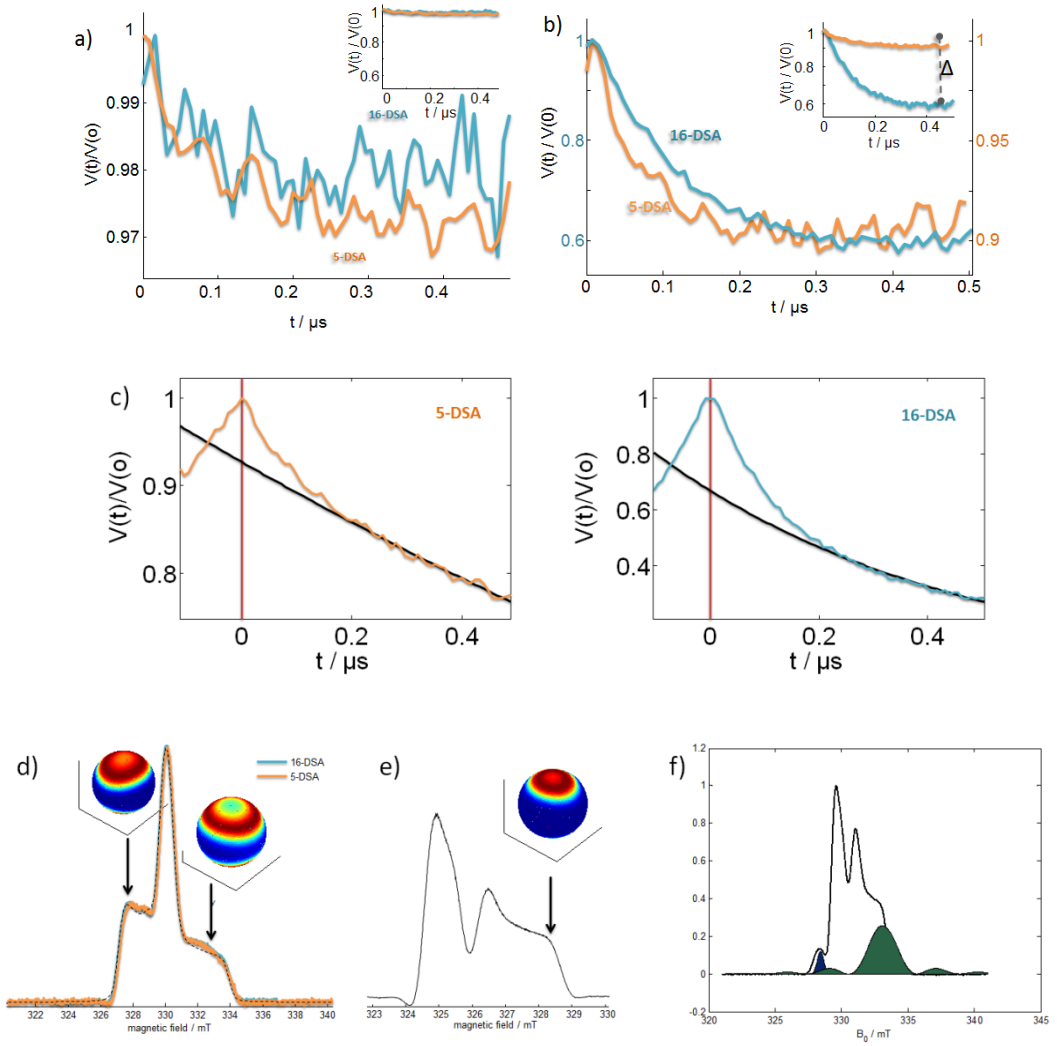

Figure S2. a) Background-corrected DEER-time traces of 4 mM 16-DSA (blue) and 5-DSA (orange) in 4 wt % de-PG4. Note that the modulation depth is less than 0.03. Therefore, one could neglect contributions of dipolar couplings of the DSA-probes among each other in the discussion of the MISS-DEER experiment, instead of subtracting them from the original time traces, shown in b). The pump- and observer-pulse position were exactly the same as indicated in Figure 2a) and S1. b) Background-corrected time-traces of the ^{14}N-^{15}N-DEER experiments (see also Fig. 2b). The inset shows the non-rescaled data. The dashed line indicated the modulation depth. The pure FS-DSA interaction was extracted from this data, subtracting the appropriately weighted time-traces shown in a). With the indicated pump and detection positions (Fig. 2 and S1) the raw time-traces yield: for 5-DSA/FS V(observed) = 0.76 V(MISS DEER) + 0.23 V(DSA-DSA DEER) + (<0.01) V(FS-FS-DEER). And for 16-DSA/FS: V(observed) = 0.62 V(MISS DEER) + 0.07 V(DSA-DSA DEER) + 0.28 V(FS-FS-DEER). c) Uncorrected, original DEER echoes of the ^{14}N-^{15}N experiments. The zero-time is marked by the red vertical line. The black curves represent the backgrounds, which were subtracted from the echoes, to yield the time-traces shown in b). d) Electron-spin-echo of 5- and 16-DSA in de-PG4. The field-positions of the pump- (highfield) and observer-pulses (lowfield) applied are marked with black arrows. The excited directions, as indicated by the red areas on the spheres above, are similar for both, 5-DSA and 16-DSA, because there is only little difference between the two echoes. The dashed line corresponds to a spectral simulation of the ESE. e) Electron-spin-echo of ^{15}N-FS. Orientations excited by the pump-pulse applied in the DEER experiments are indicated by the red colour on the sphere above. f) Excitation profiles of the applied pump- and observer-pulses. For the ^{14}N-5-DSA/^{15}N-FS the spectrum is shown and the experimental conditions are summarized in the main text (12ns pump pulse, 32 ns observer pulses, observation and pump position and 5-DSA/^{15}N-FS ratio). The contribution of ^{14}N-^{14}N distances is smaller by a factor 2.96 compared to ^{14}N-^{15}N distances. Thus, provided that both types of distances are a priori of similar probability, the DEER spectrum/distance distribution is always dominated by the heteronuclear distances. However, we have separately recorded the ^{14}N-DSA spectra under identical conditions. Subtracting this reference dipolar time trace from the MISS DEER time trace, the ^{14}N-^{15}N distances are obtained in good approximation. Note that in any case the not significant ^{14}N-^{14}N-distances show up in the reference spectrum in the accessible distance range. For ^{14}N-16-DSA/^{15}N-FS the enhancement factor of the heteronuclear distances is 1.8. Again our background correction did not indicate a significant contribution of ^{14}N-^{14}N distances.

Note that the subtracted background functions (Figure S2c)) are exponentials, corresponding to a three dimensional background. In the case of the cylindrically shaped denpols one could however expect a one or two dimensional background. Yet, our earlier work showed that for the mere FS-distribution around a denpol, subtraction of a 3D background is appropriate, due to the spatial distribution of FS around the denpols and the short contact time of FS on the denpol's surface.[1] For DSA we assume that for longer τ_2 the background function could become two or one dimensional. However, with the qualitative interpretation one can safely state that the dimensionality of the subtracted background-function does not affect the relative comparison of the FS-5-DSA and FS-16-DSA time-traces at all.

Assuming the background to be exponential in nature, uncertainties about the correct contribution of the background to the raw data have to be considered, too, since the intramolecular contributions also lead to nearly exponential form factors. However, the faster initial decay of the 5-DSA-FS trace compared to 16-DSA-FS, as well as the difference in modulation depth, remain virtually identical for all possible combinations of background contributions. Hence, uncertainties about the background subtraction do not affect qualitative interpretations.

CW-EPR

A Miniscope MS200 (Magnettech, Berlin, Germany) benchtop spectrometer was used for X-band CW EPR measurements at a microwave frequency of ~9.4 GHz. Measurements were performed at room temperature (293 K) using a modulation amplitude of 0.05 mT. The microwave frequency was recorded with a Racal-Dana frequency counter (model 2101).

Spectral Simulations

Table S1. Selected simulation parameters of 5-DSA and 16-DSA. The parameters correspond to a concentration of 1 mM DSA and 1 wt % of the respective denpol. Note that the values for species B have to be treated with caution, since it is very difficult to extract precise values of very slow tumbling nitroxides from multi-component spectra. If two species were included in a simulation, the spectral values are shown in the form: [value for species A]/[value for species B]. Note that the rotational correlation time is related to the principle values of the diffusion tensor D by: $\tau_c = 6^{-1}(D_{xx}\ D_{yy}\ D_{zz})^{-1/2}$.

	5-DSA / de-PG1	5-DSA / de-PG2	5-DSA / de-PG3	5-DSA / de-PG4
g_{iso}	2.0059	2.0058	2.0058/2.0055	2.0059/2.0055
A_{iso} / MHz	41.10	41.10	40.63/ 40.63	40.17/40.17
D /s^{-1}	$[1.1\cdot10^8\ 1.0\cdot10^8]$	$[0.7\cdot10^8\ 1.0\cdot10^8]$	$[1.5\cdot10^8\ 1.0\cdot10^7]$ / $[1.0\cdot10^7\ 2.0\cdot10^6\ 3.0\cdot10^8]$	$[1.5\cdot10^8\ 1.0\cdot10^7]$/ $[1.0\cdot10^7\ 2.0\cdot10^6\ 3.0\cdot10^8]$
	16-DSA / de-PG1	16-DSA / de-PG2	16-DSA / de-PG3	16-DSA / de-PG4
g_{iso}	2.0056	2.0057	2.0061/2.0055	2.0060/2.0055
A_{iso} / MHz	42.50	42.50	41.57/41.57	40.17/40.17
D /s^{-1}	$[1.0\cdot10^8\ 1.0\cdot10^8]$	$[1.2\cdot10^8\ 1.0\cdot10^8]$	$[2.0\cdot10^8\ 1.0\cdot10^8]$/ $[1.0\cdot10^7\ 2.0\cdot10^6\ 3.0\cdot10^8]$	$[2.2\cdot10^8\ 1.0\cdot10^8]$/ $[1.0\cdot10^7\ 2.0\cdot10^6\ 3.0\cdot10^8]$

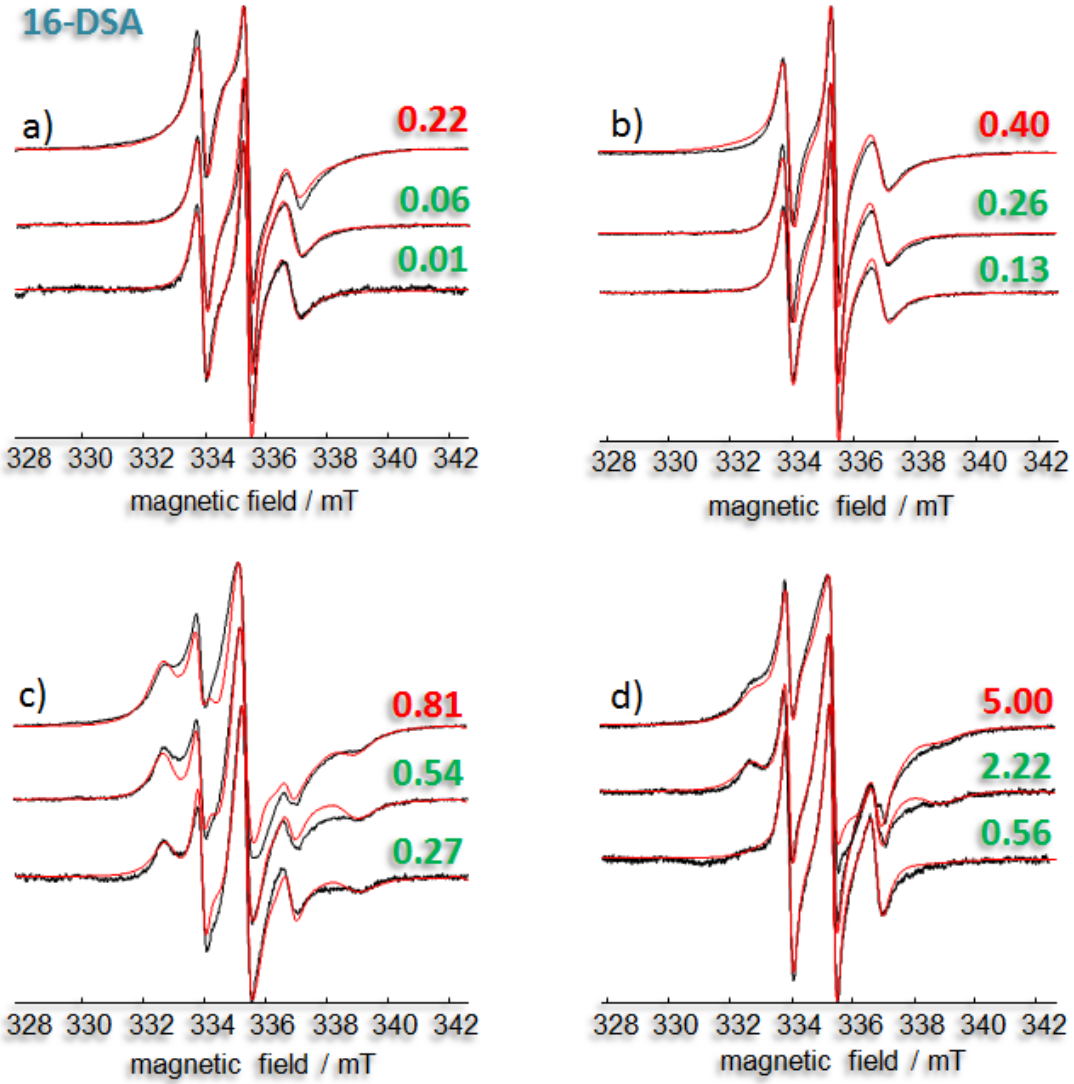

Figure S3. CW EPR spectra (black) and corresponding spectral simulations (red) for a) 1 wt % de-PG1, b) 1 wt % de-PG2, c) 1 wt % de-PG3 and d) 1 wt % de-PG4, in solution with 16-DSA. The numbers on the right of each spectrum indicate the ratio of n(16-DSA)/n(denpols monomer) in a 1 wt % solution of denpols (see Table 1 for the details on the calculations). Green indicates that the simulation includes no free or precipitated 16-DSA, red the contrary. Spectra of 16-DSA incorporated in de-PG3 or de-PG4 were simulated with two (or three) components.

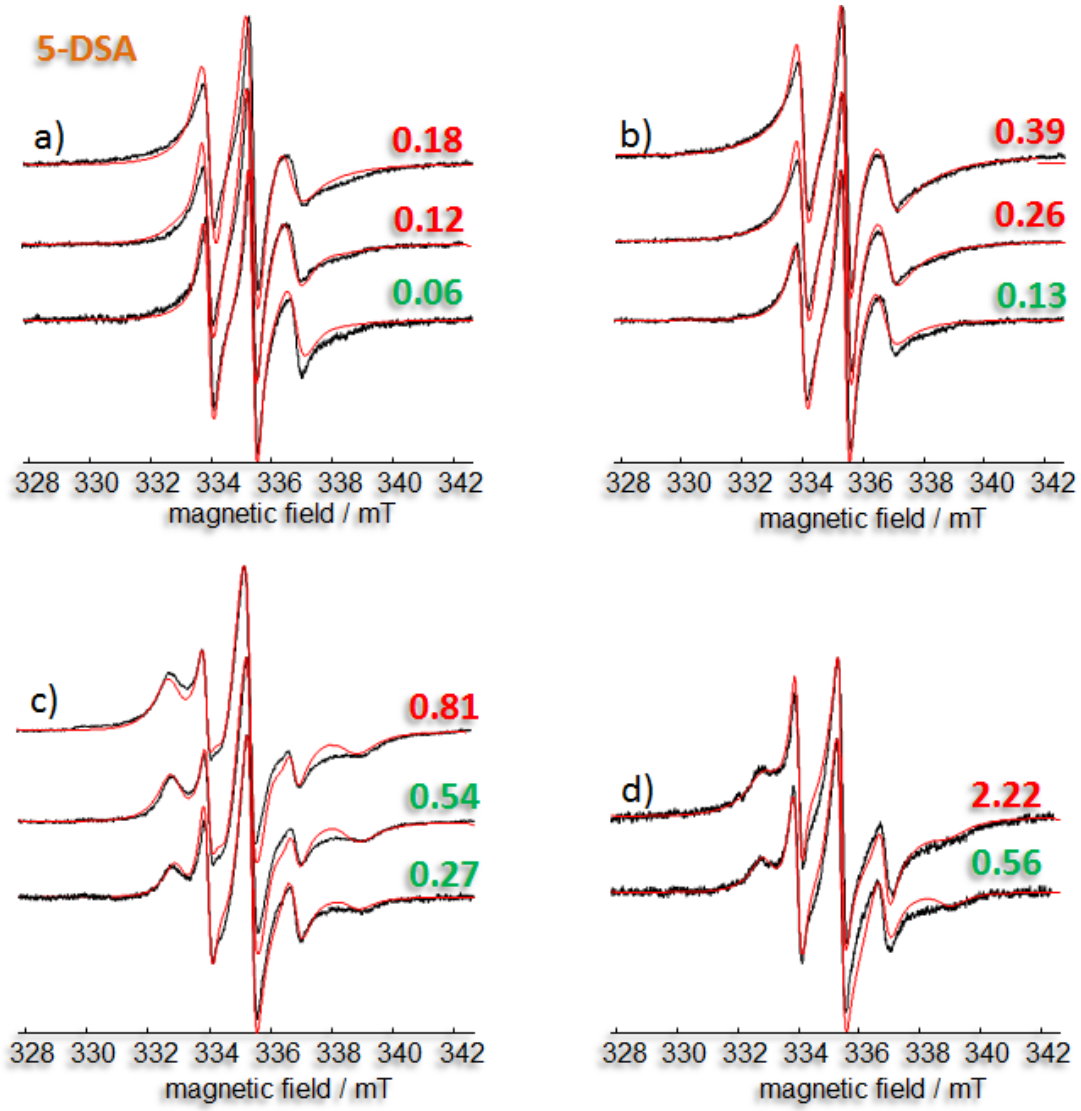

Figure S4. CW EPR spectra (black) and corresponding spectral simulations (red) of 5-DSA contained in solutions of a) 1 wt % de-PG1, b) 1 wt % de-PG2, c) 1 wt % de-PG3 and d) 1 wt % de-PG4. The numbers on the right of each spectrum indicate the ratio of n(5-DSA)/n(denpol monomers) (see Table 1 for details on the calculations). Green indicates that the simulation includes no free or precipitated 5-DSA, red the contrary. Spectra of incorporated 5-DSA and de-PG3 and 4 were simulated with two (or three) components.

Note that 5-DSA and de-PG4 at a ratio of 2.22 was simulated with only a minimal contribution of precipitated 5-DSA. Therefore, 5-DSA shows only a minimally smaller ability to incorporate into de-PG4 then 16-DSA. Therefore, 2.20 DSA molecules per denpol-monomer reported as maximal loading capacity for both probes, 16- and 5-DSA. All the other values, correspond exactly to those obtained from measurements on 16-DSA.

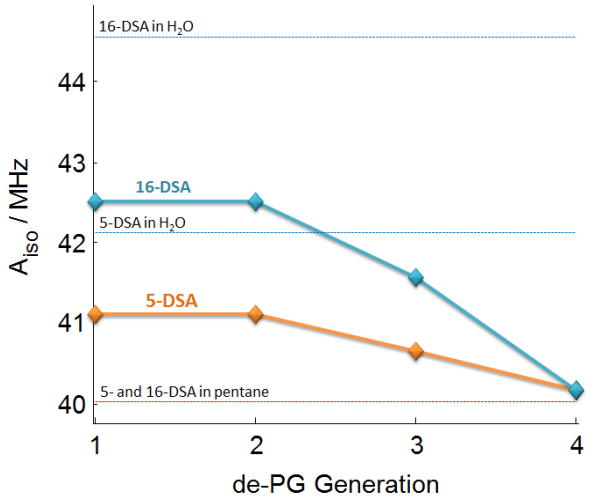

Figure S5. Isotropic hyperfine coupling constant A_{iso} of the nitroxide group of 5-DSA (orange) and 16-DSA (blue) as obtained from spectral simulations of the CW EPR data (see Figure S3 and S4) plotted versus the generation of the dendronized polymer incorporating the probe. The hfc-values of 5- and 16-DSA in pure water and pentane are indicated by the dotted blue and red lines.

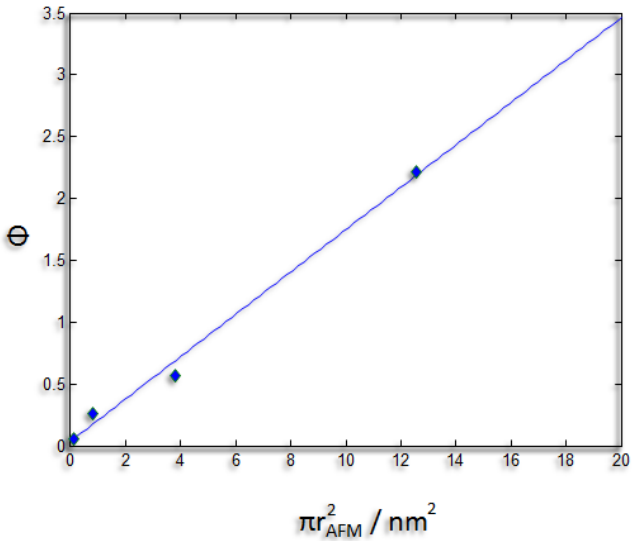

Figure S6. The loading capacity Φ (i.e. guest-molecules per denpol monomer-unit) plotted versus the area of the cylinder cross-section of the respective denpol generation (estimated based on radii from AFM tapping heights of the denpols PG1-4).[2] Assuming a constant height of the repeat units, the cross-section is directly proportional to the volume of the cylinder. Thus, the AFM radius and the loading capacity depend on the generation in the same manner. The data points for the different generations were fitted linearly: $b*(\pi r^2_{AFM})+a$, where $b = 0.17\ nm^{-2} \pm 0.01\ nm^{-2}$ and $a = 0.038 \pm 0.07$.

Molecular Structures and Supplementary EPR Data

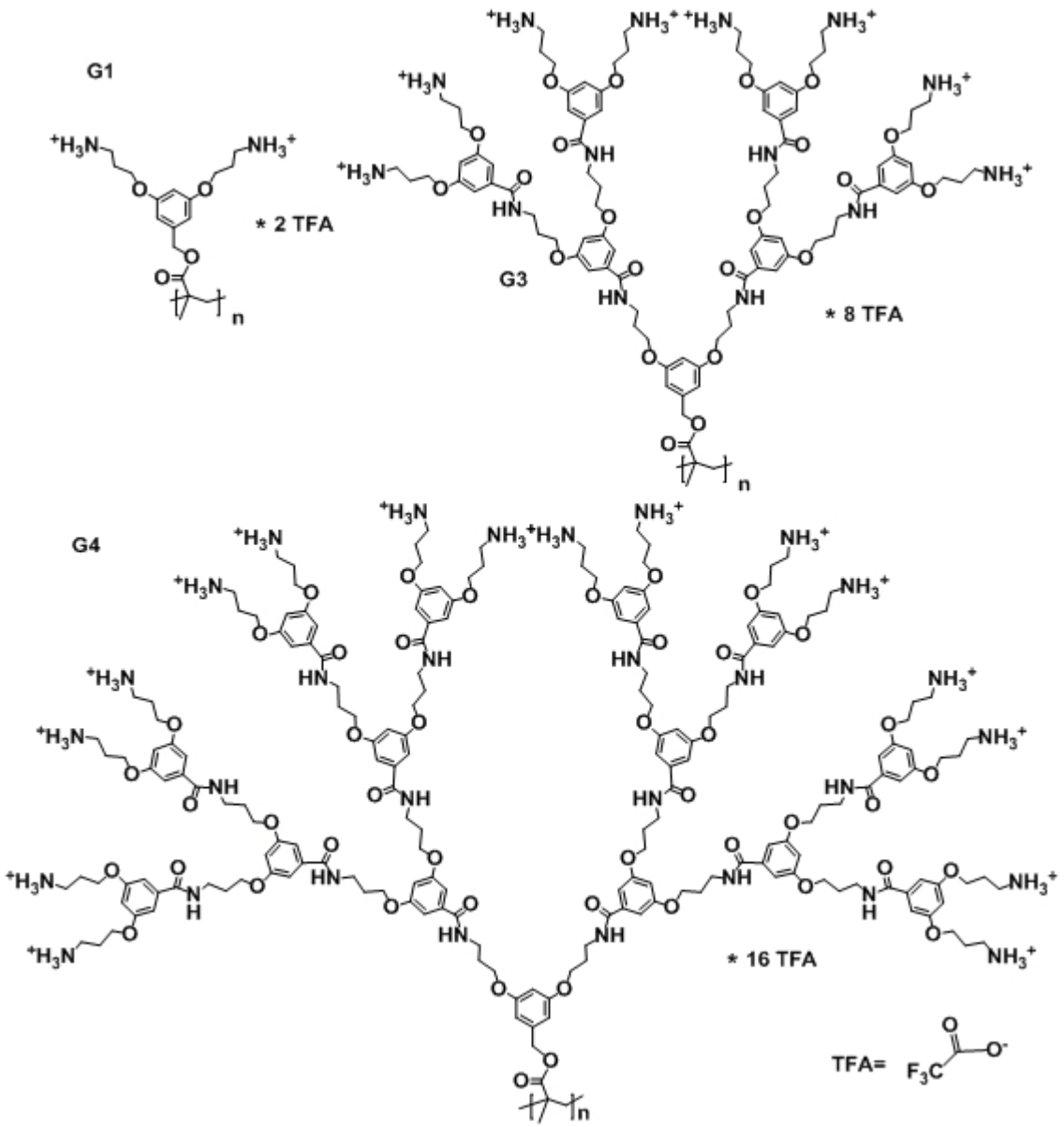

Figure S7. Molecular structure of the denpols de-PG1, de-PG3 and de-PG4; de-PG2 is depicted in Figure 1.

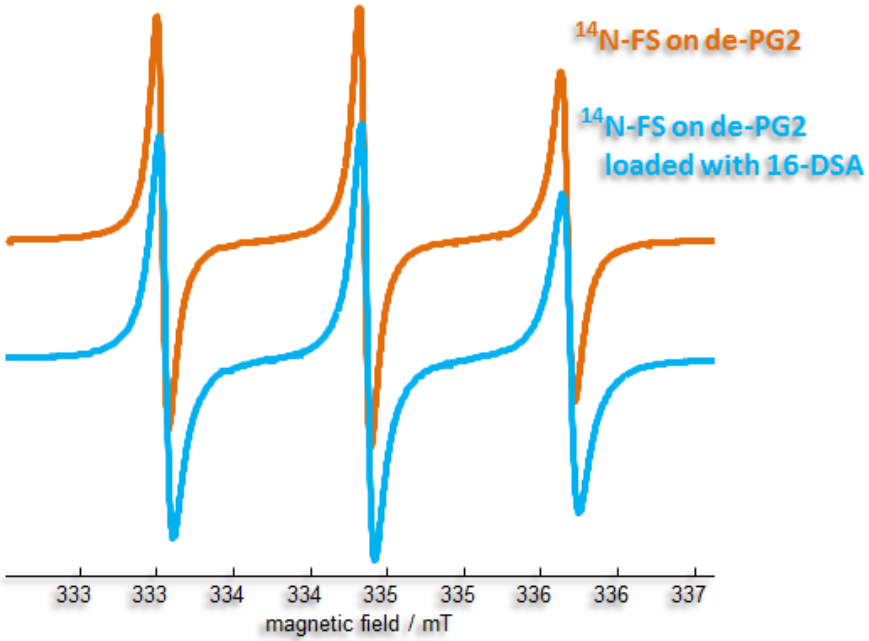

Figure S8. CW EPR spectra of 1mM ^{14}N-FS in presence of de-PG2 (yellow; for details on the coordination of FS with charged denpols see Kurzbach et al. 2011[1]) and ^{14}N-FS in presence of de-PG2 that is loaded with 1 mM 16-DSA (1 wt % aqueous solution). As can be seen, no significant differences in the spectra of FS on the loaded and the unloaded denpol occur. Hence, a coordination of DSA on the surface of the cylinder is unlikely since the hydrophobic tail would drastically affect the coordination behavior of the FS probes. Note that the spectral contribution of 16-DSA cannot be detected clearly, due significantly strong line broadening, compared to FS. Therefore, we chose 4 mM and 4 wt % denpol for the ^{14}N – ^{15}N DEER experiment, to increase the 5- and 16-DSA signal intensity.

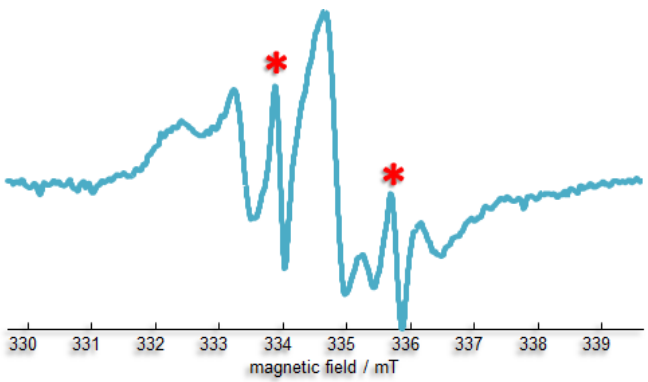

Figure S9. CW EPR spectrum of 1 mM 16-DSA and 0.1 mM ^{15}N-FS in an aqueous solution 1 wt % de-PG3. Here the superposition of both paramagnetic species is clearly visible. The lines stemming from ^{15}N-FS are marked with the red asterisks.

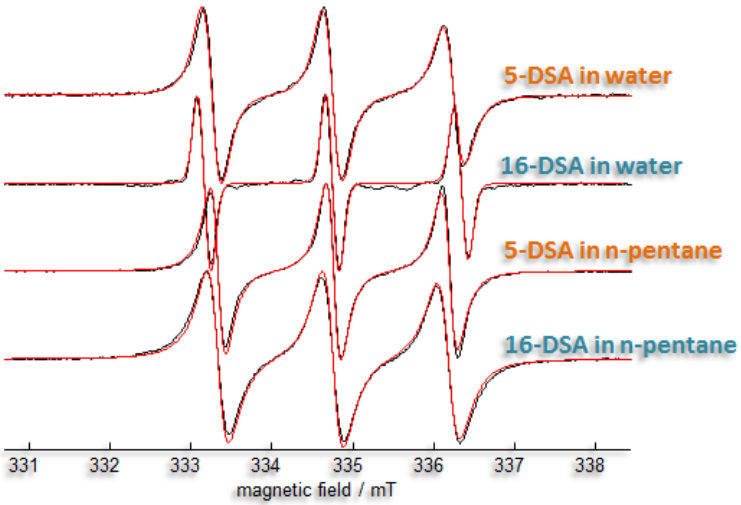

Figure S10. CW EPR spectra of 5- (orange label) and 16-DSA (blue label) are shown in black and the corresponding spectral simulations are overlaid in red. Thus, the A_{iso} values for DSA in aqueous and organic media were determined. Thereby A_{iso}-values of 42.04 MHz for 5-DSA in water, 44.65 MHz for 16-DSA in water, 40.17 MHz for 5 and 16-DSA in n-pentane were obtained, as depicted in Figure S5. The differences in A_{iso} and linewidth of 5-DSA and 16-DSA in water may be traced back to micellization of DSA in water..[3]

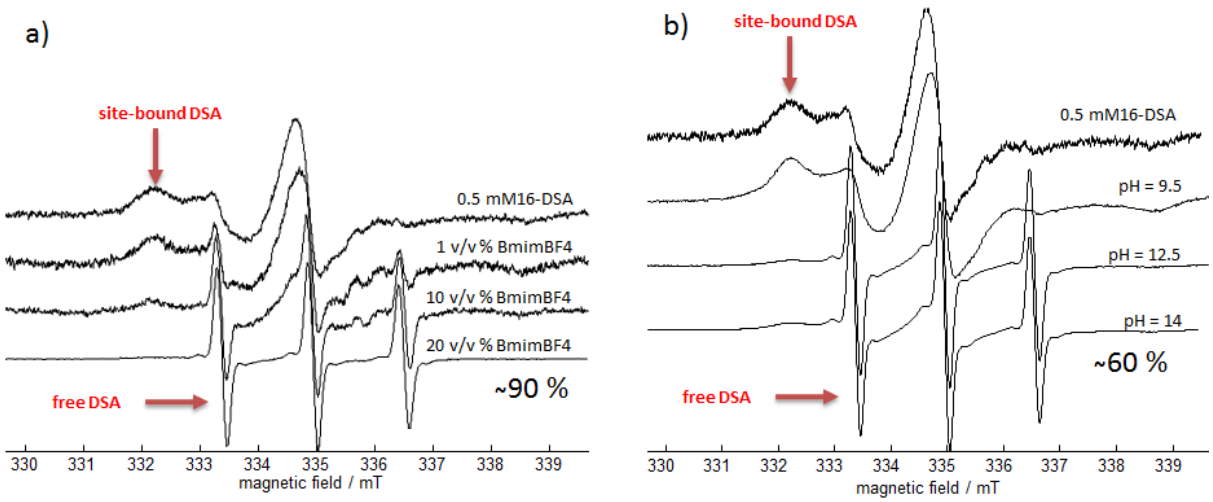

Figure S11. a) Release of 16-DSA from de-PG3 by $BmimBF_4$. Over 90% of the 16-DSA guest-molecules were released by addition of only 20 v/v % of the release agent. b) The response of 5-DSA incorporated into de-PG3 to an increasing pH. DSA is released significantly from the denpols, as the pH is raised. At pH = 12.5 most of the 16-DSA probes (approx. 60%) are release from de-PG3. No significant further release of 16-DSA is observed, when the pH is raised from 12.5 to 14. Note that the spectrum of 16-DSA in de-PG3 is strongly shifted towards the species **B**, when compared to the spectrum in Figure 1b). This might be traced back to aging of the denpol over time due to intramolecular H-bond formation and a decreasing number of looser binding sites **A** for DSA. Yet, the principle possibility to release DSA from the denpols can still be observed clearly.

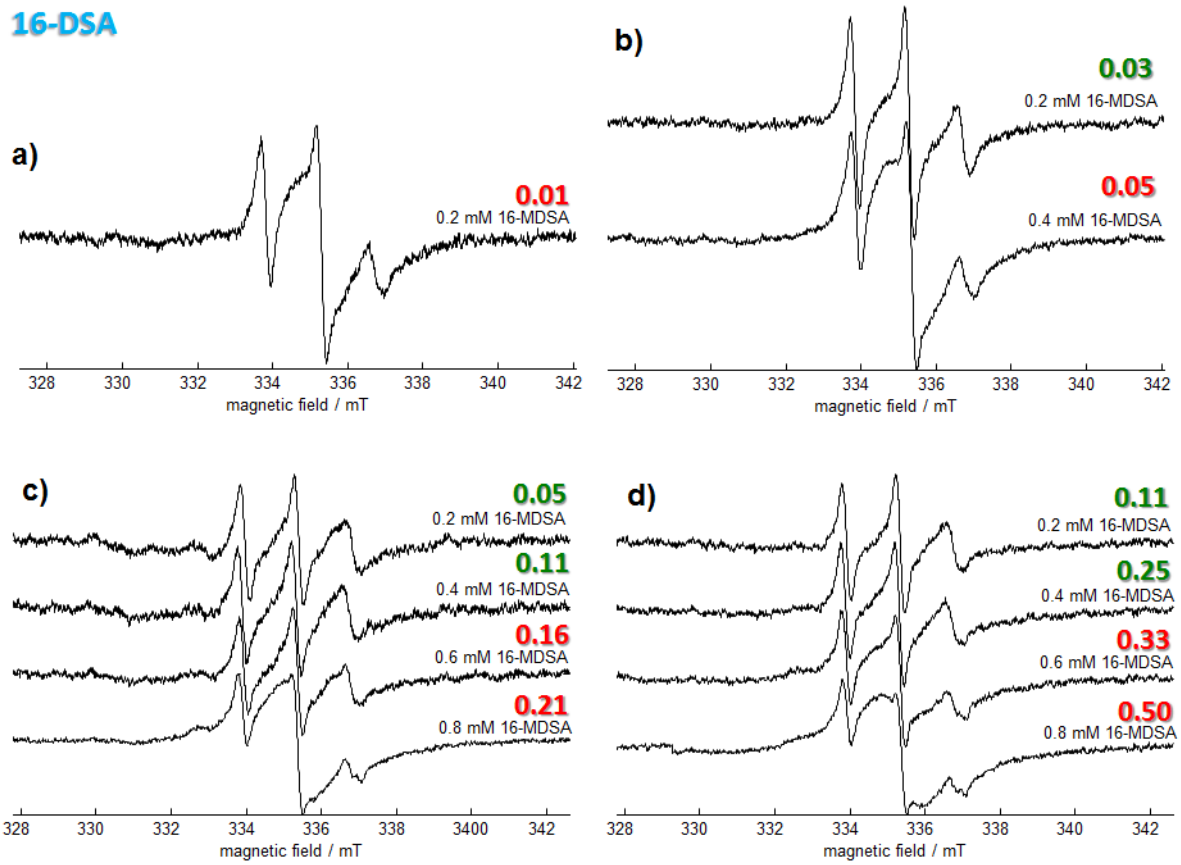

Figure S12. CW EPR spectra a) 1 wt % de-PG1, b) 1 wt % de-PG2, c) 1 wt % de-PG3 and d) 1 wt % de-PG4, together in solution with 16-methyl(M)-DSA. The numbers above the spin-probe concentration on the right of each spectrum indicate the ratio of n(16-MDSA)/n(denpols monomer) at 1 wt % solution of denpols (see Table 1 for details on the principle calculation). Green indicates that the spectra appear to feature no contribution from free or precipitated 16-MDSA, red the contrary. Simulation of the depicted spectra is hardly possible, due to the bad signal-to-noise ratio and precise, reliable values cannot be extracted from them by means of spectral simulation. Yet, from the apparent line shapes it can reliably be concluded that the amount of MDSA that can be incorporated by the denpols is much lower than the amount of not esterified DSA.

1. D. Kurzbach, D. Kattnig, B. Zhang, A. D. Schlüter and D. Hinderberger, *J. Phys. Chem. Lett.*, 2011, **2**, 1583-1587.
2. B. Zhang, R. Wepf, K. Fischer, M. Schmidt, S. Besse, P. Lindner, B. T. King, R. Sigel, P. Schurtenberger, Y. Talmon, Y. Ding, M. Kröger, A. Halperin and A. D. Schlüter, *Angew. Chem. Int. Ed.*, 2011, **50**, 737-740.
3. S. Ruthstein, R. Artzi, D. Goldfarb and R. Naaman, *Phys. Chem. Chem. Phys.*, 2005, **7**, 524-529.